5816 J. Med. Chem. 2009, 52, 5816–5825
DOI: 10.1021/jm900420c

Journal of Medicinal Chemistry Article

A Modular Platform for the Rapid Site-Specific Radiolabeling of Proteins with ^{18}F Exemplified by Quantitative Positron Emission Tomography of Human Epidermal Growth Factor Receptor 2

Herman S. Gill,[†] Jeff N. Tinianow,[†] Annie Ogasawara,[†] Judith E. Flores,[†] Alexander N. Vanderbilt,[†] Helga Raab,[‡] Justin M. Scheer,[‡] Richard Vandlen,[‡] Simon-P. Williams,[†] and Jan Marik*,[†]

[†]*Departments of Biomedical Imaging and* [‡]*Protein Chemistry, Genentech Inc., 1 DNA Way, South San Francisco, California 94080*

Received April 1, 2009

Receptor-specific proteins produced by genetic engineering are attractive as PET imaging agents, but labeling with conventional ^{18}F-based prosthetic groups is problematic due to long synthesis times, poor radiochemical yields, and low specific activities. Therefore, we developed a modular platform for the rapid preparation of water-soluble prosthetic groups capable of efficiently introducing ^{18}F into proteins. The utility of this platform is demonstrated by the thiol-specific prosthetic group, [^{18}F]FPEGMA, which was used to produce site-specifically ^{18}F-labeled protein (^{18}F-trastuzumab-ThioFab) in 82 min with a total radiochemical yield of 13 ± 3% and a specific activity of 2.2 ± 0.2 Ci/μmol. ^{18}F-trastuzumab-ThioFab retained the biological activity of native protein and was successfully validated *in vivo* with microPET imaging of Her2 expression in a xenograft tumor-bearing murine model modulated by the Hsp90 inhibitor, 17-(allylamino)-17-demethoxygeldanamycin.

Introduction

Proteins and peptides make up a large part of the armamentarium available for the molecular imaging of cell-surface biomarkers. Although the development of "ideal" imaging agents is an important goal, in practice many imaging agents are developed from existing proteins. The development of positron emission tomography (PET)[a] imaging agents from monoclonal antibodies and their engineered fragments (immuno-PET)[1] holds promise as a tool for localizing and quantifying molecular targets and may enhance the noninvasive clinical diagnosis of pathological conditions. Small immuno-PET imaging agents, such as Fab antibody fragments (50 kDa) or diabodies (paired dimers of the covalently associated V_H-V_L region of Mab, 55 kDa),[2−4] may be particularly useful since they exhibit a short circulation half-life and high tissue permeability and reach a maximum tumor to background ratio between 2−4 h after injection, facilitating the use of short half-life isotopes such as the widely available ^{18}F ($T_{1/2}$ = 109.8 min). Unfortunately, methods for introducing ^{18}F into proteins are far from satisfactory at present as relatively mild aqueous reaction conditions are necessary to preserve the function of most proteins. Hence, existing ^{18}F-labeled prosthetic groups used for protein conjugations are often limited by some combination of poor radiochemical yield, long synthesis time, and low specific activity. Improved methods for generating ^{18}F-labeled proteins may facilitate molecular imaging in humans and thereby address questions in the clinical development process: What is the level of target expression? How heterogeneous is it? And how does it change over time? Therefore, we have developed a new platform for the rapid production of ^{18}F-labeled prosthetic groups capable of efficiently introducing ^{18}F into proteins.

Two conventional techniques for incorporating ^{18}F into proteins are the modification of ε-amino groups of lysine residues and thiol groups of cysteine residues. Of these techniques, the most common method reported is the amino-specific prosthetic group, *N*-succinimidyl 4-[^{18}F]fluorobenzoate ([^{18}F]SFB).[5−12] However, [^{18}F]SFB is labile in the basic aqueous conditions generally required for efficient amino reactions,[13] providing limited yield and specific activity of the ^{18}F-labeled conjugate. Furthermore, [^{18}F]SFB often impairs the biological activity of the resulting conjugate, which may result from a combination of harsh reaction conditions and the modification of amino groups near the binding region. For example, ^{18}F-labeled anticarcinoembryonic agent (CEA) diabody was recently produced with the compromised immunoreactivity (57%) characteristic of [^{18}F]SFB conjugations.[2,9]

Site-specific protein modification, where a selected amino acid distant from the binding region is modified, is generally preferred over a random modification since it potentially provides a homogeneous product with unaltered biological activity. Proteins engineered to contain cysteine, which is relatively limited within the proteome and primarily present as a nonreactive disulfide, are well suited for the development of site-specific conjugates.[14−16] A phage display-based assay was recently developed to identify cysteine substitution sites

*To whom correspondence should be addressed: phone, 650-225-8821; fax, 650-467-7991; e-mail, marik.jan@gene.com.

[a] Abbreviations: PET, positron emission tomography; MeCN, acetonitrile, DMF, *N*,*N*-dimethylformamide; DMSO, dimethyl sulfoxide; K222, Kryptofix-222; % ID/g, percent ID per gram; CuAAC, copper-(I)-catalyzed alkyne−azide cycloaddition; BPDS, bathophenanthroline-disulfonate; TBTA, tris[(1-benzyl-1*H*-1,2,3-triazol-4-yl)methyl]amine; 17-AAG, 17-(allylamino)-17-demethoxygeldanamycin; PEG or PEG$_n$, monodisperse polyethylene glycol containing 2−10 ethylene glycol units; Her2, human epidermal growth factor receptor 2; TOF LC/MS, time-of-flight liquid chromatography/mass spectrometry; DIAD, diisopropyl azodicarboxylate; NHS, *N*-hydroxysuccinimide; ThioMab, monoclonal antibody containing engineered cysteine for site-specific modification; ThioFab, antigen binding fragment of ThioMab.

 Published on Web 09/09/2009

Scheme 1. (a) Convergent Methods for Introducing ^{18}F into Proteins Using ^{18}F-Labeled Prosthetic Groups Produced from Our Platform and (b) Radiolabeling ThioFab Fragments Using [^{18}F]FPEGMA

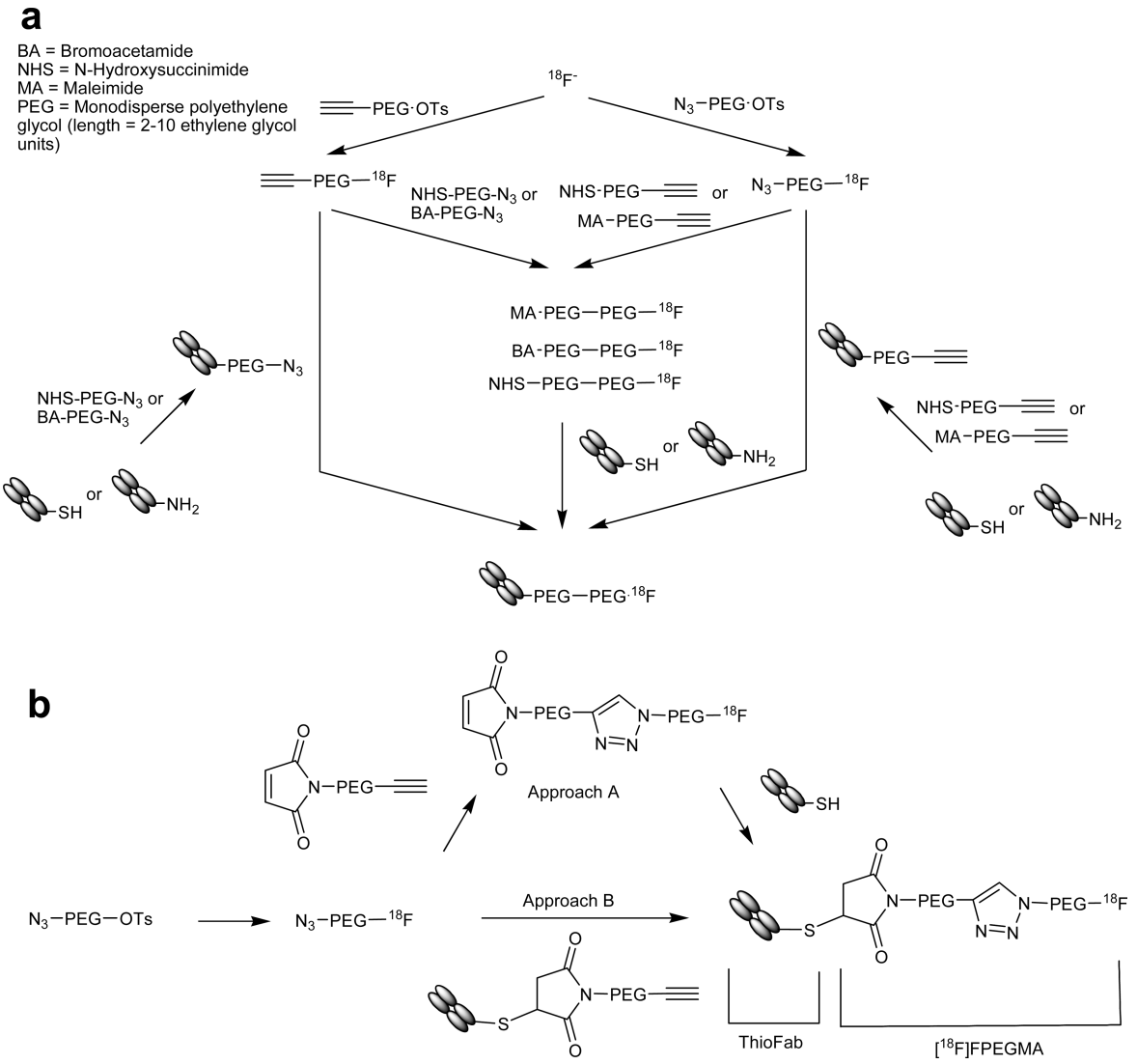

that provide superior thiol reactivity without compromising the structure and function of the conjugate.[17] The method was used to produce a monoclonal antibody (Mab) containing two reactive cysteine residues (ThioMab),[18] from which an antigen binding fragment (Fab) containing a single reactive thiol (ThioFab) is conveniently generated. This prompted the selection of trastuzumab-ThioFab, which is derived from trastuzumab containing a V110C mutation (Kabat numbering) in the light chain (trastuzumab-ThioMab), for the development of site-specific ^{18}F-labeled conjugates.

Prosthetic groups containing maleimide, such as [^{18}F]FBEM,[19] [^{18}F]FBAM,[20] [^{18}F]FBABM,[15,21] [^{18}F]FBOM,[22] [^{18}F]FDG-MHO,[23] and [^{18}F]FPyMe,[24] may be used to site-specifically introduce ^{18}F into a thiol-bearing protein. [^{18}F]FBEM, [^{18}F]FBAM, [^{18}F]FBABM, and [^{18}F]FBOM were developed from a common platform where the aromatic precursor, ^{18}F-fluorobenzaldehyde ([^{18}F]FBAl), was coupled to an aminooxy-bearing maleimide precursor. However, the presence of aromatic and (with the exception of [^{18}F]FBOM) aliphatic moieties enhances the lipophilicity of these prosthetic groups which may limit the conjugation efficiency for thiol groups located in a hydrophilic environment. Moreover, these prosthetic groups require long synthesis times and typically provide limited radiochemical yields of ^{18}F-labeled protein. A similar platform using the widely available radiotracer [^{18}F]FDG instead of [^{18}F]FBAl was proposed for the production of the water-soluble maleimide-bearing prosthetic group, [^{18}F]FDG-MHO. However, [^{18}F]FDG requires a longer synthesis time and provides a lower radiochemical yield than [^{18}F]FBAl.

An alternative platform using silicon-based fluoride acceptor (SiFA) synthons was recently investigated for the development of ^{18}F-labeled organosilicon prosthetic groups, such as the thiol-bearing Si[^{18}F]FA-SH[25] and Si[^{18}F]FA-isothiocyanate.[26] The SiFA platform sets a high standard for total synthesis time and ease of synthesis primarily by eliminating the requirement for HPLC purification. However, the SiFA synthon is highly lipophilic which necessitates the use of organic cosolvent and may potentially alter the pharmacokinetic properties of the radiolabeled biomolecule.

These limitations inspired the development of a new platform to robustly produce ^{18}F-labeled prosthetic groups with diverse physicochemical properties (Scheme 1a). The foundation of this platform is the copper(I)-catalyzed azide−alkyne cycloaddition (CuAAC).[27,28] Since the CuAAC is orthogonal to most functional groups, the development of varied prosthetic groups is readily achieved

by coupling modular "building blocks" containing azide or alkyne functionalities (Scheme 2). Although previously used for the preparation of ^{18}F-radiolabeled peptides,[29] our platform is the first reported set of methods to use the CuAAC to introduce ^{18}F into proteins.

A compelling example of our platform is the maleimide-bearing prosthetic group, [^{18}F]FPEGMA, which was rapidly produced in a single reaction vessel by a two-step synthesis (Scheme 1b, approach A). Moreover, polyethylene glycol (PEG) based building blocks were used to promote the water solubility and conjugation efficiency of [^{18}F]FPEGMA with protein in aqueous conditions. [^{18}F]FPEGMA was evaluated as a prosthetic group with trastuzumab-ThioFab, and the resulting conjugate (^{18}F-trastuzumab-ThioFab) was validated *in vivo* as an imaging agent of the Her2 expression level in a human tumor xenograft murine model modulated by the Hsp90 inhibitor, 17-(allylamino)-17-demethoxygeldanamycin (17-AAG).[30,31] Her2, a receptor tyrosine kinase of the epidermal growth factor family, is an important target for the development of breast cancer therapeutics, and the inhibition of the chaperone protein Hsp90, which is responsible for maintaining the stability of a variety of oncoproteins including Her2, is a promising therapeutic mode.

Although the development and biological validation of [^{18}F]FPEGMA is primarily considered, the production of a variety of ^{18}F-labeled prosthetic groups from our platform was also investigated (Scheme 1a). This includes the thiol-specific bromoacetamide compound [^{18}F]FPEGBA, the amino-specific *N*-hydroxysuccinimide (NHS) compound [^{18}F]FPEGNHS, the azide-specific compound [^{18}F]FPEG-propargyl, and the alkyne-specific compound [^{18}F]FPEGN$_3$. Furthermore, important recommendations are provided for the general development of ^{18}F-labeled products from our platform.

Scheme 2. Alkynes and Azides Used as Building Blocks for Preparation of ^{18}F-Prosthetic Groups Using CuAAC

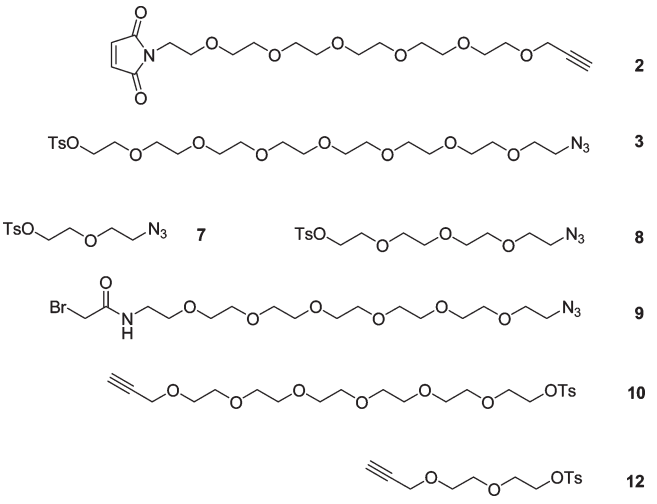

Results

Synthesis of Building Blocks. A set of heterobifunctional polyethylene glycol based building blocks for constructing ^{18}F-labeled prosthetic groups was prepared (Scheme 2). The details for the synthesis of precursors needed to prepare [^{18}F]FPEGMA ([^{18}F]**5**) are outlined in Scheme 3. The synthesis of **2** from hexaethylene glycol required two steps; the Williamson ether synthesis using equimolar amounts of NaH and propargyl bromide provided a 54% yield of propargyl-PEG$_6$-OH (**1**), which was reacted with excess maleimide by the PPh$_3$/DIAD-mediated Mitsunobu reaction providing a 25% yield of **2**. Compound **3** was obtained from commercially available heterobifunctional HO-PEG$_8$-N$_3$ and tosyl chloride in pyridine with a 25% yield. Azides **7** and **8** were synthesized in 30% and 19% yields, respectively, by heating equimolar amounts of NaN$_3$ and the appropriate PEG-ditosylate in DMF to 110 °C. Bromoacetamide **9** was prepared from commercially available NH$_2$-PEG$_7$-N$_3$ and bromoacetyl bromide. Compound **10** was prepared from **1**, and compound **12** was obtained in two steps from diethylene glycol with propargyl-PEG$_2$-OH (**11**) as a monopropargylated intermediate. The synthetic procedures for compounds **1**−**6** are presented in the Experimental Section and the preparation of intermediates **7**−**12** is described in detail in the Supporting Information.

Microwave-Assisted Nucleophilic ^{18}F-Fluorination. Tetrabutylammonium hydrogen carbonate (TBAHCO$_3$) was selected over a Kryptofix-222/K$_2$CO$_3$ (K222/K$_2$CO$_3$) system as a phase transfer catalyst for the nucleophilic ^{18}F-fluorination, including [^{18}F]FPEG$_2$N$_3$ (prepared from **7**), [^{18}F]FPEG$_4$N$_3$ (from **8**), and [^{18}F]FPEG$_8$N$_3$ ([^{18}F]**4**, obtained from **3**). Since TBAHCO$_3$ exhibited higher thermal stability relative to K222/K$_2$CO$_3$, microwave heating at high temperatures accelerated the azeotropic removal of water to less than 5 min. Additionally,

Scheme 3. Synthesis of [^{18}F]**5** and ^{18}F-Labeled trastuzumab-ThioFab ([^{18}F]**6**, [^{18}F]FPEGMA-trastuzumab-ThioFab)[a]

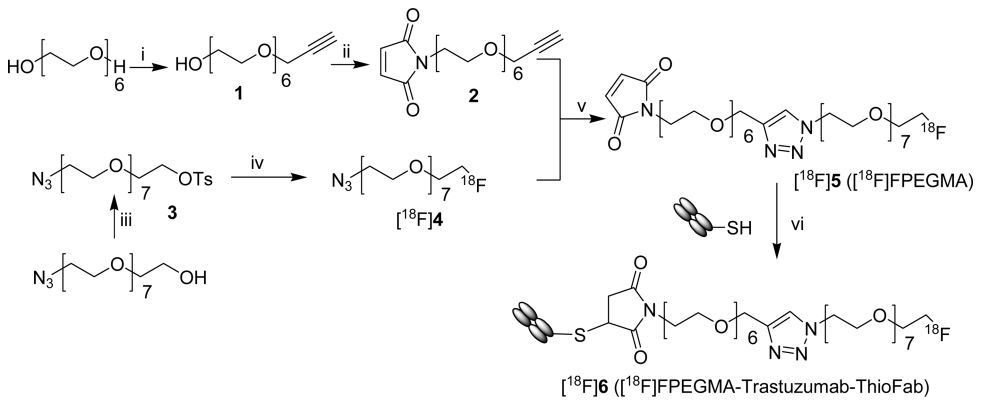

[a] Reaction conditions: (i) NaH, propargyl bromide; (ii) maleimide, PPh$_3$, DIAD; (iii) TsCl, pyridine; (iv) TBAHCO$_3$, [^{18}F]fluoride; (v) CuSO$_4$·5H$_2$O, BPDS, sodium ascorbate; (vi) phosphate buffer, pH 8.

Table 1. Comparison of Three Methods for the CuAAC of [^{18}F]**4** and **2**, Including Reaction Time, Conversion from [^{18}F]**4** to [^{18}F]**5**, and Purity of Crude [^{18}F]**5** with Respect to ^{18}F-Labeled Breakdown Products

method	catalysts	time (min)	% conversion	% purity
A	$CuSO_4$/ascorbate	20	79	66
B	$CuSO_4$/ascorbate/BPDS	1	96	89
C	$Cu(MeCN)_4PF_6$/TBTA/2,6-lutidine	5	100	90

microwave heating provided a high ^{18}F-fluorination efficiency (89.0 ± 1.8%, n = 4) in 3 min for [^{18}F]**4** in acetonitrile, with similar yields observed for [^{18}F]$FPEG_4N_3$. Decreased yields of [^{18}F]$FPEG_2N_3$, which is volatile in the fluorination and evaporation conditions employed, were prevented by using resealable reaction vessel caps and gentle evaporation conditions.

Optimization of the CuAAC and the Preparation of [^{18}F]5 ([^{18}F]FPEGMA). Three catalytic systems were evaluated for the reaction of [^{18}F]**4** and **2** using the CuAAC (Table 1). Method A, which employs $CuSO_4 \cdot 5H_2O$ and sodium ascorbate as a source of Cu^I,[29,32] provided the desired product in 20 min with a 79% conversion efficiency and a 66% purity. The long reaction time and limited purity observed prompted the investigation of ligands capable of accelerating the CuAAC. Method B adds the Cu^I ligand, bathophenanthrolinedisulfonate (BPDS), to method A which reduced the reaction time to 1 min, increased the conversion efficiency to 96%, and improved the purity of crude [^{18}F]**5** to 89%. For methods A and B, the formation of ^{18}F-labeled degradation products was decreased when the synthesis of [^{18}F]**4** was catalyzed by $TBAHCO_3$ compared to $K222/K_2CO_3$ and when [^{18}F]**4** was purified with an Alumina N light cartridge prior to the CuAAC (data not shown).

Method C employs acetonitrile-compatible reagents such as $Cu(MeCN)_4PF_6$ as a source of Cu^I, tris[(1-benzyl-1*H*-1,2,3-triazol-4-yl)methyl]amine (TBTA) as a Cu^I ligand, and 2,6-lutidine as a base.[33,34] Using method C, the reaction time (less than 5 min), purity of crude [^{18}F]**5** (90%), and conversion efficiency (100%) were comparable to method B. Furthermore, alumina purification of [^{18}F]**4** prior to the CuAAC reaction did not impact the purity of crude [^{18}F]**5** and was omitted from method C.

After HPLC purification and SPE treatment, method B provided [^{18}F]**5** with a yield of 61 ± 4%, a radiochemical purity of 94% (Supporting Information Figure 1a), and a specific activity of 5.6 ± 1.6 Ci/μmol (determined against an HPLC standard curve of ^{19}F-labeled **5**) in 47 ± 2 min (n = 4). The identity of [^{18}F]**5** was confirmed by HPLC coelution with ^{19}F-labeled standard (Supporting Information Figure 1b) and by LC/MS analysis of the decayed product. The lipophilicity (log P) of [^{18}F]**5** was −2.41 ± 0.09.

Conjugation of [^{18}F]5 to trastuzumab-ThioFab. The conjugation efficiency of [^{18}F]**5** and trastuzumab-ThioFab was tested as a function of protein concentration, pH, and time (Table 2). As the protein concentration and pH were increased, reduced conjugation time and increased efficiency were observed. The degradation of [^{18}F]**5** and aggregation of trastuzumab-ThioFab were comparable at pH 6.5 and 8.

The purification of ^{18}F-trastuzumab-ThioFab was performed on a NAP-5 desalting column or a Bio-Sep S-2000 SEC-HPLC column (system D). The NAP-5 method provided coelution of unconjugated [^{18}F]**5** with trastuzumab-ThioFab, particularly for reactions with a low conjugation efficiency. The Bio-Sep S-2000 SEC-HPLC separated ^{18}F-trastuzumab-ThioFab from ^{18}F-labeled aggregates and [^{18}F]**5** (and ^{18}F-labeled degradation products). The purified final product, ^{18}F-trastuzumab-ThioFab, was analyzed by HPLC system A (Supporting Information Figure 2b), system C (Supporting Information Figure 2a), and TOF LC/MS. The optimized conjugation procedure provided ^{18}F-trastuzumab-ThioFab in 30 ± 7% conjugation efficiency, with greater than 90% radiochemical purity, and a specific activity of 2.2 ± 0.2 Ci/μmol (n = 5). The total synthesis time was 82 ± 4 min from the start of synthesis, and the total decay corrected yield was 13 ± 3%.

Table 2. Conjugation Efficiency of [^{18}F]**5** (5 mCi, 1 nmol) to trastuzumab-ThioFab (100 μg, 2 nmol) against Protein Concentration, pH, and Time[a]

		yield (%)		
pH	protein concn (mg/mL)	10 min	30 min	60 min
6.5	0.5	26	39	44
6.5	1.0	26	42	53
6.5	2.0	47	66	74
7.2	1.0	64	74	77
8.0	1.0	79	85	85

[a] 10 mCi fractions of [^{18}F]**5** (in acetonitrile after SPE treatment) were dispensed into ten reaction vials and evaporated, after which trastuzumab-ThioFab was added.

Hsp90 Targeted Therapy and MicroPET Imaging. Mice were distributed into two groups (n = 4) according to tumor uptake and volume as determined by ^{18}F-trastuzumab-ThioFab 1 day prior to 17-AAG treatment. 17-AAG was administered to the treated group at day 0, while the control group was left untreated. PET imaging with ^{18}F-trastuzumab-ThioFab was performed at day 1 (14 h after the administration of the last 17-AAG dose), day 5, and day 7. Coronal slices through the tumor of control and 17-AAG-treated groups 1 day before and 1 day after therapy are shown in Figure 1a. The average tumor uptake in control and treated groups over a 1 week period is shown in Figure 1b, and the uptake in selected tissues is listed in Table 3. PET imaging at day 1 revealed a significant reduction in tumor uptake (0.65 ± 0.09% ID/g) compared to the control group (1.33 ± 0.14% ID/g, P = 0.00046) and the uptake in the treated group measured before therapy (1.31 ± 0.13% ID/g, P = 0.00012) (Table 3). The correction for nonspecific uptake using muscle as a reference tissue provided a 70% decrease in ^{18}F-trastuzumab-ThioFab tumor uptake after therapy. The renal clearance of ^{18}F-trastuzumab-ThioFab was predominant with high uptake in the renal cortex and accumulation of radioactivity in the bladder (Table 3). Although tracer retention in the liver was relatively low, the hepatobiliary route contributed to tracer excretion with radioactive metabolites accumulating in the gall bladder and large intestine.

Discussion

Important development considerations for [^{18}F]FPEGMA include the use of water-soluble building blocks derived from PEG precursors, assembly of building blocks by the CuAAC, and optimization of the site-specific conjugation

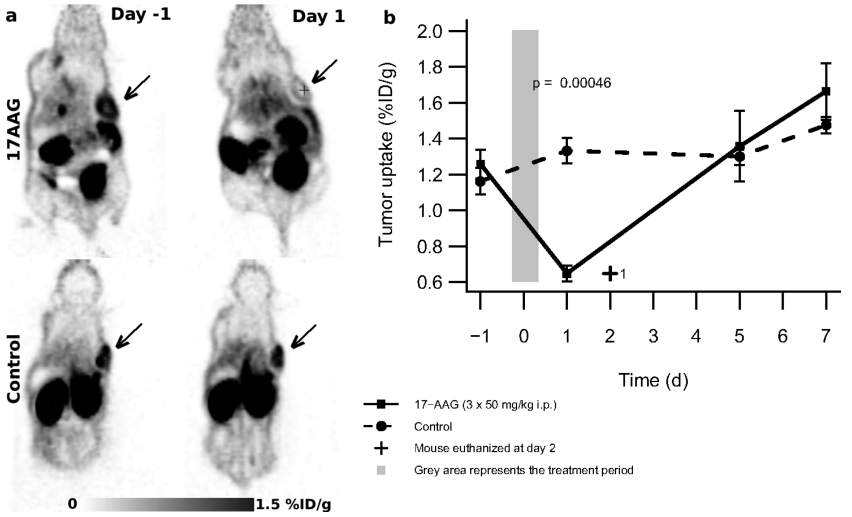

Figure 1. (a) Representative microPET images (coronal slices through tumor) before (day −1) and after (day 1) 17-AAG therapy (top) compared to a nontreated animal (bottom). (b) Tumor uptake of ^{18}F-trastuzumab-ThioFab for treated and control groups over 7 days.

Table 3. Average Uptake of ^{18}F-trastuzumab-ThioFab in Select Tissues before (day −1) and after (days 1, 5, and 7) Treatment with 17-AAG[a]

	uptake (% ID/g)			
17-AAG treated tissue	day −1	day 1	day 5	day 7
bladder	90.76 ± 23.40	63.05 ± 23.08	57.89 ± 9.11	47.11 ± 32.10
blood	0.80 ± 0.06	1.31 ± 0.23	0.97 ± 0.04	0.67 ± 0.07
brain	0.08 ± 0.01	0.12 ± 0.02	0.08 ± 0.01	0.06 ± 0.01
gall bladder	3.59 ± 1.43	4.05 ± 1.86	3.58 ± 0.32	1.97 ± 0.71
kidney	15.26 ± 3.02	20.54 ± 4.97	20.48 ± 6.47	23.92 ± 6.98
large intestine	3.96 ± 2.05	4.05 ± 1.47	3.54 ± 1.61	4.19 ± 0.97
liver	0.62 ± 0.06	0.97 ± 0.08	0.82 ± 0.10	0.54 ± 0.04
muscle	0.29 ± 0.03	0.33 ± 0.04	0.25 ± 0.02	0.21 ± 0.04
skin	0.44 ± 0.09	0.50 ± 0.05	0.48 ± 0.02	0.37 ± 0.04
tumor	1.31 ± 0.13	0.65 ± 0.09	1.36 ± 0.34	1.66 ± 0.27

[a] Kidney uptake was measured in the cortex, and blood uptake was measured in the left ventricle. Data are presented as mean ± SD.

to trastuzumab-ThioFab with subsequent biological validation.

The development of a new synthetic platform to produce ^{18}F-labeled prosthetic groups for protein conjugations emerged from our unsuccessful application of the lipophilic prosthetic group, [^{18}F]FBAM, to trastuzumab-ThioFab. From this observation, we hypothesized that hydrophilic prosthetic groups would provide superior conjugation kinetics and efficiency with trastuzumab-ThioFab and potentially other hydrophilic proteins. Therefore, building blocks derived from PEG precursors were investigated to improve water solubility while maintaining solubility in organic solvents conventionally employed for nucleophilic ^{18}F-fluorination. Prosthetic groups derived from our platform (Scheme 1a) were more water-soluble than compounds derived from the [^{18}F]FBAl platform. For example, the measured log *P* of [^{18}F]**5** (−2.41 ± 0.09) is three units lower (more hydrophilic) than the value reported for [^{18}F]FBOM and over five units lower than [^{18}F]FBAM.[22] Our hypothesis was validated since the conjugation efficiency of [^{18}F]**5** to trastuzumab-ThioFab was dramatically superior to [^{18}F]FBAM under comparable conditions.

Perhaps the most compelling design consideration of [^{18}F]FPEGMA and of our platform in general is the assembly of azide and alkyne-bearing building blocks by the CuAAC. Three CuAAC methods were developed to optimize the yield of [^{18}F]**5** (Table 1). Method A provided a 79% conversion of starting material [^{18}F]**4** in 20 min; however, the purity of crude [^{18}F]**5** was only 66%, which subsequently diminished due to the instability of [^{18}F]**5** in the reaction conditions employed. The low preparative yield (less than 20%) provided by method A prompted the investigation of Cu^{I} ligands, such as BPDS and TBTA, which are known to increase the CuAAC reaction rate and may further enhance the orthogonality of the CuAAC.[33,35,36] Method B, which adds BPDS to the reaction system of method A, provided a dramatic improvement to the reaction time, conversion, purity (Table 1), and preparative yield (61%) of [^{18}F]**5**. Using method B, the purity of crude [^{18}F]**5** diminished after 1 min, which may be attributed to the sensitivity of the maleimide moiety to hydrolysis in basic aqueous conditions.

The limited stability of [^{18}F]**5** in the aqueous conditions of method A or B prompted the development of method C, which was performed in anhydrous acetonitrile. Method C provided a higher conversion and more sustainable purity of crude [^{18}F]**5** over time compared to method B. Moreover, [^{18}F]**5** was stable in the presence of basic species, such as $TBAHCO_3$ and 2,6-lutidine, in anhydrous conditions obviating the alumina treatment between the ^{18}F-fluorination and CuAAC reaction steps. Method C also provided a higher yield than method B for reactants with limited water solubility, such as [^{18}F]FPEG$_2$N$_3$, and for products which are labile in aqueous conditions, such as [^{18}F]FPEGNHS. However, method B was selected for the preparation of [^{18}F]**5** due to the extremely short period of time needed to obtain nearly quantitative conversion. Nevertheless, a consistent radiochemical process

Scheme 4. Amino-Reactive Prosthetic Group ^{18}FPEGNHS and Thiol-Reactive Prosthetic Group ^{18}FPEGBA

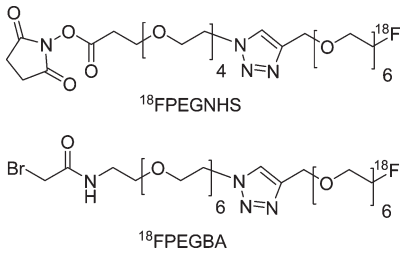

may be applied when producing varied ^{18}F-labeled prosthetic groups by either method B or method C. This has strong implications for automation since a common reaction platform eliminates the dedication of a synthesis module for a specific prosthetic group, such as [^{18}F]SFB.

The orthogonality of the CuAAC enabled the development of multiple prosthetic groups capable of introducing ^{18}F into proteins (Scheme 1a). Method C was used to produce [^{18}F]FPEGNHS (Scheme 4) from a commercially available precursor (N_3-PEG_4-NHS), and the product was subsequently conjugated to the Fab fragment of trastuzumab (trastuzumab-Fab, Supporting Information). [^{18}F]FPEGNHS may limit the reduction in immunoreactivity characteristic of amino-specific modifications through a combination of high specific activity and limited steric hindrance within the binding region (smaller building blocks are under development). Therefore, [^{18}F]-FPEGNHS has strong potential as an alternative to [^{18}F]SFB for performing amino-specific modifications. We have also developed the thiol-specific compound, [^{18}F]-FPEGBA (Scheme 4), using method B (Supporting Information); however, the conjugation efficiency of [^{18}F]-FPEGBA with trastuzumab-ThioFab at pH 8 was insufficient for routine application.

The CuAAC was also used to directly label proteins with [^{18}F]FPEG-propargyl and [^{18}F]FPEGN_3 (Scheme 1b, approach B), reducing the synthesis of ^{18}F-labeled protein to two radiochemical steps and providing an alternative method for site-specific modification. For example, preliminary tests reacting [^{18}F]**4** with propargyl-PEG_6-trastuzumab-ThioFab provided conjugation efficiencies up to 15% (Supporting Information). A similar method was employed to couple [^{18}F]$FPEG_3$-propargyl to an azide-PEG-modified nanoparticle with a high conjugation efficiency due to the presence of multiple azide sites.[37] This highlights the high conjugation efficiency and specific activity possible for ^{18}F-labeled proteins since multiple azide or alkyne groups can be positioned on a protein without cross-reactivity. However, since the combination of Cu^{II} and ascorbate tends to degrade proteins,[38] the CuAAC methods that we have developed are not directly applicable to proteins. Instead, we continue to investigate methods including Cu^{I} with the rigorous exclusion of oxygen, Cu^{II} mixed with reducing agents, or Cu^{I} associated with BPDS which may enhance the bioorthogonality of the CuAAC with proteins.[39] Nevertheless, [^{18}F]FPEG-propargyl and [^{18}F]FPEGN_3 have demonstrated promising results as prosthetic groups for the development of ^{18}F-labeled peptides using method B with minor modifications (Supporting Information).

The site-specific conjugation of [^{18}F]**5** to trastuzumab-ThioFab was optimized with respect to the reactant stability and reaction rate. Regarding the stability of thiol-bearing proteins, which generally decreases as pH and protein concentration increase, the formation of trastuzumab-ThioFab dimers or aggregates did not increase across the range of pH (6.5−8) and protein concentration (1−2 mg/mL) tested (Table 2). Regarding the stability of [^{18}F]**5** during the conjugation reaction, the formation of degradation products was also independent of pH across the range tested (Table 2) or during scaled-up production. Although [^{18}F]**5** was stable during small-scale conjugations (using 10 mCi to generate Table 2), significant product degradation was observed during scaled-up production (more than 200 mCi) which limited the conjugation efficiency (Supporting Information Figure 2c). The dependence of [^{18}F]**5** degradation on total radioactivity coupled with the formation of a broad spectrum of byproducts may indicate that [^{18}F]**5** is susceptible to radiolysis which is characteristic for maleimide compounds.[40,41] Irrespective of the decomposition mechanism, the conjugation conditions were selected to maximize the reaction rate while ensuring that limited aggregates are formed. Considering the pH independence of the reactants' stability, basic conditions (pH 8) provided acceptable conjugation efficiency (30%) for ^{18}F-trastuzumab-ThioFab. However, the complete degradation of [^{18}F]**5** ultimately reduced the conjugation efficiency and specific activity of ^{18}F-trastuzumab-Thio-Fab. Despite this limitation, a high specific activity of ^{18}F-trastuzumab-ThioFab was obtained, which may reduce the potential for receptor saturation and improve target uptake, particularly for cells with low receptor density. Notably, the yield (13%), specific activity (2.2 ± 0.2 Ci/μmol), and total synthesis time (82 ± 4 min) of ^{18}F-trastuzumab-ThioFab are favorable when compared against ^{18}F-labeled anti-CEA diabody (1.4% yield and 0.05 Ci/μmol specific activity in 173 min using [^{18}F]SFB).[9]

After optimizing the conjugation of [^{18}F]**5** to trastuzumab-ThioFab, the biological activity of ^{18}F-trastuzumab-ThioFab was validated by Scatchard analysis. The affinity of the conjugate (K_D = 11.9 ± 2.3 nM) was comparable to native trastuzumab-ThioFab (9.6 ± 1.2 nM). Additionally, trastuzumab-ThioFab retained a comparable binding affinity to the parent trastuzumab-Fab (8.3 ± 1.0 nM), indicating that the modification of trastuzumab-ThioFab with [^{18}F]**5** did not alter its Her2 binding properties. Further biological validation of ^{18}F-trastuzumab-ThioFab included a treatment response study of a Her2-overexpressing tumor xenograft in a murine model modulated by the Hsp90 inhibitor, 17-AAG.

The effect of the Hsp90 inhibitor, 17-AAG, on Her2-positive tumors has been characterized.[42] Immuno-PET was recently employed to monitor the effect of 17-AAG on Her2 expression level *in vivo* using a ^{68}Ga-labeled DOTA-conjugated Herceptin F(ab′)$_2$ fragment (^{68}Ga-DCHF).[30,31] Smith-Jones measured a 70% reduction in Her2 levels lasting 5 days followed by a return to pretreatment levels after 12 days. These data suggest that ^{68}Ga-DCHF is capable of monitoring tumor response to 17-AAG treatment earlier than ^{18}FDG PET. However, the short half-life of ^{68}Ga ($T_{1/2}$ = 68 min) is not well suited for the plasma half-life of F(ab)′$_2$, resulting in a signal loss during the 3 h period required prior to PET acquisition. Therefore, improved imaging properties were expected by coupling a shorter plasma half-life species, such as monovalent Fab fragments, with an appropriate radionuclide, such as ^{18}F[3].

A consistent response in Her2 levels to 17-AAG was observed whether measured by ^{18}F-trastuzumab-ThioFab (Figure 1) or ^{68}Ga-DCHF.[30,31] The 70% decrease in tumor uptake of ^{18}F-trastuzumab-ThioFab observed after therapy was identical to that measured by Smith-Jones using ^{68}Ga-DCHF.[30]

Additionally, since ^{18}F-trastuzumab-ThioFab (Figure 1a) was imaged only 1 half-life after injection, the image quality may compare favorably to ^{68}Ga-DCHF (imaged 3 half-lives after injection).

In summary, we have developed a modular platform for the facile preparation of ^{18}F-labeled prosthetic groups assembled from building blocks using the CuAAC reaction. The application of our platform was demonstrated by [^{18}F]FPEGMA, which was used to site-specifically modify trastuzumab-ThioFab. Generally, the methods described herein for producing ^{18}F-radiolabeled proteins provide high radiochemical yields and specific activity with a short synthesis time. ^{18}F-trastuzumab-ThioFab is a viable alternative to ^{68}Ga-DCHF for the treatment response monitoring of Her2 levels. Ultimately, our platform may be an important tool for the discerning radiochemist and may simplify radiochemical process development by providing a reliable, convenient, and consistent method for producing diverse ^{18}F-labeled prosthetic groups.

Experimental Section

General. Solvents and chemicals were purchased from Aldrich (Milwaukee, WI) unless stated otherwise. Heterobifunctional polyethylene glycols were purchased from Iris Biotech (Marktredwitz, Germany), and N_3-PEG_8-NHS was purchased from Quanta Biodesign (Powell, OH). Egg phospholipid was purchased from Avanti Polar lipids (Alabaster, AL), and 17-(allylamino)-17-demethoxygeldanamycin (17-AAG) was obtained from InvivoGen (San Diego, CA). [^{18}F]Fluoride was purchased from PETNET Solutions (Palo Alto, CA), ^{18}F trap and release columns (8 mg) were purchased from ORTG, Inc. (Oakdale, TN), and Strata-X 60 mg cartridges were purchased from Phenomenex (Torrance, CA). The following reversed-phase HPLC systems were used to determine purity and purify the products. System A: Phenomenex Jupiter C18 300 Å (150 × 4.6 mm, 5 μm), 0.05% TFA + 10−90% acetonitrile, 0−7 min, 90% acetonitrile, 7−10 min, 2 mL/min. System B: Phenomenex Luna C18 (250 × 10 mm, 5 μm) 0.05% TFA + 20% acetonitrile, 7 mL/min. System C: Phenomenex BioSep-SEC-S 2000 (300 × 4.60 mm, 5 μm) 50 mM PBS, pH 7.2, 0.5 mL/min. System D: Phenomenex BioSep-SEC-S 2000 (300 × 7.80 mm, 5 μm) 20 mM PBS, pH 7.2, 1.0 mL/min. System E: Altima C-18 (100 × 22.0 mm, 5 μm) 0.05% TFA + 10−60% acetonitrile, 0−30 min, 24 mL/min. System F: Agilent Eclipse XDB-C18 (150 × 4.6 mm, 5 μm) 0.05% TFA + 10−90% acetonitrile, 0−10 min, 1 mL/min, 50 °C. The analytical and semipreparative HPLC systems used for radiochemistry were equipped with an UV absorbance and radioactivity detector (PMT); the purity of radioactive products was determined by detecting UV absorbance at 214, 254, and 280 nm and radioactivity. Mass spectrometry and purity analysis of low molecular weight products were performed on a PE Sciex API 150EX LC-MS system equipped with an Onyx Monolithic C_{18} column. The purity of low molecular weight compounds determined at UV 214 and 254 nm was ≥95% if not stated otherwise. LC-MS analysis of proteins was performed on a PRLP-S, 1000 Å, microbore column (50 mm × 2.1 mm; Polymer Laboratories, Palo Alto, CA) heated to 75 °C coupled to a TSQ Quantum Triple quadrupole mass spectrometer with extended mass range (Thermo Electron, Waltham, MA). A linear gradient from 30% to 40% B (solvent A, 0.05% TFA in water; solvent B, 0.04% TFA in acetonitrile) was used, and the eluant was directly ionized using the electrospray source. Data were collected by the Xcalibur data system and analyzed using ProMass (Novatia, Monmouth Junction, NJ). NMR spectra were recorded on a Bruker Avance II 500 or a Bruker Avance II 400 spectrometer at 298 K. The ^{1}H and ^{13}C chemical shifts are reported relative to TMS, and the ^{19}F chemical shifts are reported using TFA as an external reference standardized to −78.5 ppm. A Model 521 microwave heater (Resonance Instruments, Skokie, IL) was used for radiochemical reactions. TBTA was synthesized according the previously published procedure in 40% yield.[33] The lipophilicity (log *P*) was measured at pH 7.4 using a previously described method suitable for radiopharmaceuticals.[43]

3,6,9,12,15,18-Hexaoxahenicos-20-yn-1-ol (1). Sodium hydride, 60% dispersion in mineral oil (0.86 g, 21.4 mmol), was added in portions to the solution of hexaethylene glycol (5.5 g, 19.4 mmol) in anhydrous THF (40 mL) at 0 °C. The reaction mixture was stirred at 0 °C for 15 min, and then propargyl bromide, 80% in toluene (2.4 mL, 21.4 mmol), was added dropwise. The mixture was allowed to warm to room temperature and stirred for 3 h. The formed sodium bromide was removed by filtration, and the solvent was evaporated. The crude product was purified on a SiO_2 column using a 0−100% methanol/dichloromethane gradient to yield 3.4 g (54%) of colorless oil. ^{1}H NMR (500 MHz, $CDCl_3$) δ 2.45 (t, J = 2.4 Hz, 1H), 2.74 (br s, 1H), 3.61−3.71 (m, 24H), 4.21 (d, J = 2.4 Hz, 2H); ^{13}C NMR (100.6 MHz, $CDCl_3$) δ 58.4, 61.7, 69.1, 70.3−70.6, 72.5, 74.5, 79.7; MS ESI (m/z) $[M + H]^+$ calcd for $C_{15}H_{29}O_7$, 321.38; found, 321.4.

1-(3,6,9,12,15,18-Hexaoxahenicos-20-yn-1-yl)-2,5-pyrroledione (2). Diisopropyl azodicarboxylate (0.73 mL, 3.43 mmol) was added dropwise into the ice-cooled solution of **1** (1000 mg, 3.12 mmol), triphenylphosphine (900 mg, 3.43 mmol), and maleimide (456 mg, 4.70 mmol) in anhydrous THF (20 mL) under nitrogen atmosphere. The resulting brown solution was allowed to warm to room temperature and was stirred for 1 h at room temperature. The solvent was evaporated at a reduced pressure, and the crude product was purified on a SiO_2 column using a 0−100% hexanes/ethyl acetate gradient to yield 650 mg of yellow oil which was subsequently purified by semipreparative HPLC (system E) to provide 310 mg (25%) of colorless oil product free of triphenylphosphine oxide. ^{1}H NMR (400 MHz, $CDCl_3$) δ 2.43 (t, J = 2.36 Hz, 1H), 3.60−3.72 (m, 24H), 4.20 (d, J = 2.37 Hz, 2H), 6.70 (s, 2H); ^{13}C NMR (100.6 MHz, $CDCl_3$) δ 37.2, 58.4, 67.8, 69.1, 70.1, 70.4−70.6, 74.5, 79.7, 134.1, 170.6; MS ESI (m/z) $[M + H]^+$ calcd for $C_{19}H_{30}NO_8$, 400.19; found, 400.0.

23-Azido-3,6,9,12,15,18,21-heptaoxatricos-1-yl *p*-Toluenesulfonate (3). The solution of 23-azido-3,6,9,12,15,18,21-heptaoxatricosan-1-ol (800 mg, 2.02 mmol) in pyridine (4 mL) was added dropwise to the solution of toluenesulfonyl chloride (771 mg, 4.04 mmol) and 4-dimethylaminopyridine (100 mg) in pyridine (10 mL) at room temperature. The mixture was stirred for 24 h at room temperature. The solvent was evaporated, and the crude product was purified on a SiO_2 column using a 0−100% hexanes/ethyl acetate gradient, followed by a 0−100% ethyl acetate/methanol gradient, and then purified on a semipreparative HPLC (system E) to yield 280 mg (25%) of colorless oil. ^{1}H NMR (400 MHz, $CDCl_3$) δ 2.45 (s, 3H), 3.38 (t, J = 5.02 Hz, 2H), 3.58−3.70 (m, 28H), 4.16 (t, J = 5.00 Hz, 2H), 7.34 (d, J = 8.4 Hz, 2H), 7.80 (d, J = 8.4 Hz, 2H); ^{13}C NMR (100.6 MHz, $CDCl_3$) δ 21.6, 50.7, 68.7, 69.2, 70.0, 70.5−70.8, 128.0, 129.7, 133.1, 144.7; MS ESI (m/z) $[M + H]^+$ calcd for $C_{23}H_{39}N_3O_{10}S$, 549.24; found, 549.9.

23-Azido-1-fluoro-3,6,9,12,15,18,21-heptaoxatricosane (4). The 23-azido-3,6,9,12,15,18,21-heptaoxatricosan-1-ol (500 mg, 1.26 mmol) was dissolved in DCM (2 mL) and cooled to −10 °C. DAST (0.48 mL, 3.78 mmol) was added in portions to the cooled solution, and the resulting mixture was stirred at −10 °C for 30 min, then allowed to warm to room temperature, and stirred for an additional 20 h. The excess of DAST was quenched with methanol (5 mL), and the solvents were subsequently evaporated at a reduced pressure. The oily residue was dissolved in water (3 mL) and adjusted to pH 5 using $NaHCO_3$. The crude product was purified by semipreparative HPLC (system E) to yield 122 mg (24%) of yellowish oil. ^{1}H NMR (500 MHz, $CDCl_3$) δ 3.39 (t, J = 5.0 Hz, 2H), 3.65−3.68 (m, 26H), 3.75 (dt, J = 4.2 Hz, 29.6 Hz, 2H), 4.56 (dt, J = 4.0 Hz, 47.5 Hz, 2H); ^{13}C NMR (125.7 MHz,

$CDCl_3$) δ 50.8, 70.1, 70.4, 70.5, 70.7−70.8, 70.9, 83.2 (d, J = 169 Hz); ^{19}F NMR (470.6 MHz, $CDCl_3$) δ −225.9; MS ESI (m/z) $[M + H]^+$ calcd for $C_{16}H_{33}FO_7N_3$, 398.2; found, 398.0.

1-(1-Fluoro-3,6,9,12,15,18,21-heptaoxatricos-23-yl)-4-(1-(2,5-pyrrolidone-1-yl)-3,6,9,12,15,18-hexaoxanonadeca-19-yl)-1,2,3-triazole (5, FPEGMA). $Cu(MeCN)_4PF_6$ (7.5 mg, 0.02 mmol) dissolved in acetonitrile (0.1 mL) was added at room temperature to the solution of **2** (8.0 mg, 0.02 mmol), **4** (8.0 mg, 0.02 mmol), 2,6-lutidine (2.5 mL, 0.02 mmol), and TBTA (2.0 mg, 0 004 mmol) in acetonitrile (0.2 mL). The resulting mixture was stirred for 22 h at room temperature and then diluted with water to 4 mL, and the formed precipitate was removed by filtration. The filtrate containing the product was purified by semipreparative HPLC (system E) to provide 7.5 mg (47%) of colorless oil. ^{1}H NMR (500 MHz, $CDCl_3$) δ 3.58−3.80 (m, 50H), 3.87 (t, J = 4.5 Hz, 2H), 4.53 (t, J = 5.0 Hz, 2H), 4.55 (dt, J = 47.3, 4.2 Hz, 2H), 4.68 (s, 2H), 6.70 (s, 2H), 7.73 (s, 1H); ^{13}C NMR (125.7 MHz, $CDCl_3$) δ 37.2, 50.3, 64.7, 67.9, 69.5, 69.7, 70.2, 70.6−70.7, 70.9, 83.2 (d, J = 169 Hz), 123.8, 134.2, 145.0, 170.7; ^{19}F NMR (470.6 MHz, $CDCl_3$) δ −225.8; MS ESI (m/z) $[M + H]^+$ calcd for $C_{35}H_{62}FO_{15}N_7$,797.4; found, 797.4; HPLC (system A) retention time 2.91 min.

1-[^{18}F]Fluoro-3,6,9,12,15,18-hexaoxahenicos-20-azide ([^{18}F]4). [^{18}F]Fluoride was eluted from a T&R cartridge into a 4 mL v-vial using 10 μL of 1.3 M $TBAHCO_3$ in 0.6 mL of acetonitrile/water 2:1 (v/v). Water was azeotropically removed by microwave heating at 60 W, 120 °C, under a stream of argon (600 cm^3) followed by the addition of anhydrous acetonitrile (4 × 0.7 mL). Precursor **3** (2 mg, 3.6 μmol) dissolved in acetonitrile (0.6 mL) was added, and the mixture was microwave heated in a septum-sealed vessel at 40 W, 120 °C, for 3 min. The reaction mixture was cooled to room temperature, and the crude product was used with only partial or without any further purification for CuAAC as described in the next paragraph. HPLC-based radiochemical yield of [^{18}F]**4** was 86 ± 8% and HPLC retention time 7.5 min (system F).

1-(1-[^{18}F]Fluoro-3,6,9,12,15,18,21-heptaoxatricos-23-yl)-4-(1-(2,5-pyrrolidone-1-yl)-3,6,9,12,15,18-hexaoxanonadeca-19-yl)-1,2,3-triazole ([^{18}F]5, [^{18}F]FPEGMA). Method A. The reaction mixture containing crude [^{18}F]**4** was passed across a Sep-Pak Alumina N light cartridge, the product [^{18}F]**4** was eluted with acetonitrile (0.5 mL), the solvent was evaporated to near dryness, and vial was cooled to 30 °C. Compound **2** (4 mg, 10.0 μmol) dissolved in acetonitrile (0.2 mL) was added to [^{18}F]**4**, followed by a solution of freshly prepared sodium ascorbate (7.5 mg, 40 μmol) in 0.1 mL of Tris buffer, pH 8, and $CuSO_4 \cdot 5H_2O$ (2.2 mg, 8 μmol) in Tris buffer, pH 8 (0.2 mL). The resulting brown-orange solution was stirred at room temperature for 20 min, followed by the addition of H_2O with 0.1% TFA (1 mL), and delivered to the HPLC loop for purification.

Method B. The reaction mixture containing crude [^{18}F]**4** was passed across a Sep-Pak Alumina N light cartridge, the product [^{18}F]**4** was eluted with acetonitrile (0.5 mL), the solvent was evaporated to near dryness, and the vial was cooled to 30 °C. Compound **2** (4 mg, 10.0 μmol) dissolved in acetonitrile (0.2 mL) was added to [^{18}F]**4**, followed by freshly prepared sodium ascorbate (7.5 mg, 40 μmol) in 0.1 mL of Tris buffer, pH 8, and a mixture of $CuSO_4 \cdot 5H_2O$ (2.2 mg, 8 μmol) and bathophenanthrolinedisulfonate (BPDS) (4.4 mg, 8 μmol) in Tris buffer, pH 8 (0.2 mL). The resulting brown-orange solution was stirred at room temperature for 1 min, followed by the addition of H_2O with 0.1% TFA (1 mL), and delivery to the HPLC loop for purification.

Method C. The reaction mixture containing crude [^{18}F]**4** was evaporated to near dryness (no alumina treatment required). Compound **2** (4 mg, 10.0 μmol) dissolved in acetonitrile (0.1 mL) was added, followed by a freshly prepared mixture of $Cu(MeCN)_4PF_6$ (3 mg, 8 μmol), TBTA (4.3 mg, 8 μmol), and 25 μL of 2,6-lutidine in acetonitrile (0.2 mL). The resulting light yellow solution was stirred for 5 min at room temperature, concentrated to 100 μL, diluted with H_2O with 0.1% TFA (1 mL), and delivered to the HPLC loop for purification.

Workup Procedure for Methods A−C. The crude product [^{18}F]**5** was purified by semipreparative HPLC (system B) with a retention time of 15−18 min. The collected fraction was promptly diluted to 20 mL with H_2O and loaded on a Phenomenex Strata-X 60 mg SPE cartridge, and the product trapped on the cartridge was rinsed with H_2O (10 mL), flushed with air, eluted with acetonitrile (0.5 mL) into a 1 mL v-vial, and evaporated at 30 °C to near dryness with 600 cm^3 of argon. MS ESI (m/z) $[M + H]^+$ calcd for $C_{35}H_{62}FO_{15}N_7$, 797.4; found, 797.4; HPLC (System A) retention time 2.98 min (Supporting Information Figure 1a).

[^{18}F]FPEGMA-trastuzumab-ThioFab (6). Trastuzumab-ThioFab (1.0 mg, 21 nmol) in 100 mM sodium phosphate, pH 8 (0.5 mL, 2 mg/mL), was added to [^{18}F]**5** and shaken on a test tube rocker for 10 min. The crude product was purified by a semipreparative SEC-HPLC column (system D, 10−12 min retention time) and, if necessary, concentrated to desired volume by centrifugation on an Amicon 10 kDa membrane. HPLC (system A) retention time 3.3 min (Supporting Information Figure 2b); SEC HPLC (system C) retention volume 3.0 mL (Supporting Information Figure 2a).

17-AAG Formulation and Administration. Egg phospholipid (0.5 g) in DCM (5 mL) was transferred into a 500 mL round-bottom flask, the solvent was evaporated, and the residue was stored at the reduced pressure for 16 h to remove remaining solvent. The 5% (m/v) solution of dextrose (25 mL) was added to the dried phospholipids, and the mixture was sonicated for 30 min at room temperature to obtain a milky emulsion. 17-AAG (25 mg) was dissolved in DMSO (1 mL) from which an aliquot (0.25 mL) was mixed with the egg phospholipid emulsion (4.8 mL) and sonicated at room temperature for 15 min. The resulting emulsion was administered within 30 min of preparation by intraperitoneal injection in three 1 mL doses (50 mg/kg each) over a 24 h period as described previously.[30,31]

Animal Mmodel. Beige nude XID mice of age 6−8 weeks were obtained from Harlan Sprague-Dawley (Livermore, CA). Three days prior to cell inoculation, the mice were implanted (sc, left flank) with 0.36 mg, 60 day sustained release 17β-estradiol pellets (Innovative Research of America) to maintain serum estrogen level. Mice were inoculated in the mammary fat pad with 5 × 10^6 BT474M1 cells in 50% phenol red-free matrigel. BT474M1 is a subclone of breast cancer cell line BT474 that was obtained from California Pacific Medical Center. Animal care and treatment followed protocols approved by Genentech's Institutioned Animal Care and Use Committee which is accredited by the Association for Assessment and Accreditation of Laboratory Animal Care (AAALAC).

MicroPET Imaging. The images were acquired on a microPET Focus 120 scanner (Siemens Preclinical Solutions). Mice were anesthetized with 3% sevoflurane and inoculated iv via the tail vein catheter with 0.3−0.4 mCi of ^{18}F-trastuzumab-ThioFab in isotonic solution (50−100 μL). The animals were allowed to recover on a heated blanket until ambulatory and then returned to the cage. After 2 h of conscious uptake the animals were anesthetized with 3% sevoflurane and placed head-first, prone position on the scanner bed. Body temperature was measured by a rectal probe and maintained by warm air. Dynamic 60 min scans were acquired. Full body image reconstructions were obtained using maximum a posteriori algorithm (MAP), and maximum intensity projections (MIPs) were created with ASIPro software (CTI Molecular Imaging). MAP reconstructed images were used to obtain quantitative activity levels (presented as % ID/g) in each organ of interest using ASIPro software (CTI Molecular Imaging).

Statistical Analysis. The graphs were constructed with R software version 2.4.1 (R Foundation for Statistical Computing, Vienna, Austria). Statistical significance was determined using a two-tailed Student's t-test, and P values of less than 0.05 were considered significant; data are presented as mean ± SEM if not stated otherwise.

Acknowledgment. We thank Nina Aggarwal for acquiring mass spectrometry data, Elizabeth Luis for performing Scatchard affinity analysis, George Dutina's and Phil Hass' groups for help with expression and purification of trastuzumab-ThioMab, Jagath Reddy Junutula for providing the trastuzumab-ThioMab construct, and Nick van Bruggen, Joan Greve, Leslie Khawli for insightful discussions.

Supporting Information Available: Synthetic protocols for additional building blocks **7**−**12**, method for preparation of ^{18}FPEGNHS and ^{18}FPEGBA, procedure for preparation of ThioFabs, optimized method for labeling peptides using CuAAC, method for direct conjugation of **4** to proteins using CuAAC, and supplementary Figures 1 and 2. This material is available free of charge via the Internet at http://pubs.acs.org.

References

(1) van Dongen, G. A.; Visser, G. W.; Lub-de Hooge, M. N.; de Vries, E. G.; Perk, L. R. Immuno-PET: a navigator in monoclonal antibody development and applications. *Oncologist* **2007**, *12*, 1379–1389.
(2) Shively, J. E. ^{18}F labeling for immuno-PET: where speed and contrast meet. *J. Nucl. Med.* **2007**, *48*, 170–172.
(3) Williams, L. E.; Wu, A. M.; Yazaki, P. J.; Liu, A.; Raubitschek, A. A.; Shively, J. E.; Wong, J. Y. Numerical selection of optimal tumor imaging agents with application to engineered antibodies. *Cancer Biother. Radiopharm.* **2001**, *16*, 25–35.
(4) Holliger, P.; Hudson, P. J. Engineered antibody fragments and the rise of single domains. *Nat. Biotechnol.* **2005**, *23*, 1126–1136.
(5) Vaidyanathan, G.; Bigner, D. D.; Zalutsky, M. R. Fluorine-18-labeled monoclonal antibody fragments: a potential approach for combining radioimmunoscintigraphy and positron emission tomography. *J. Nucl. Med.* **1992**, *33*, 1535–1541.
(6) Vaidyanathan, G.; Zalutsky, M. R. Labeling proteins with fluorine-18 using N-succinimidyl 4-[^{18}F]fluorobenzoate. *Int. J. Radiat. Appl. Instrum. B* **1992**, *19*, 275–281.
(7) Vaidyanathan, G.; Zalutsky, M. R. Improved synthesis of N-succinimidyl 4-[^{18}F]fluorobenzoate and its application to the labeling of a monoclonal antibody fragment. *Bioconjugate Chem.* **1994**, *5*, 352–356.
(8) Wester, H. J.; Hamacher, K.; Stocklin, G. A comparative study of N.C.A. fluorine-18 labeling of proteins via acylation and photochemical conjugation. *Nucl. Med. Biol.* **1996**, *23*, 365–372.
(9) Cai, W.; Olafsen, T.; Zhang, X.; Cao, Q.; Gambhir, S. S.; Williams, L. E.; Wu, A. M.; Chen, X. PET imaging of colorectal cancer in xenograft-bearing mice by use of an ^{18}F-labeled T84.66 anti-carcinoembryonic antigen diabody. *J. Nucl. Med.* **2007**, *48*, 304–310.
(10) Grierson, J. R.; Yagle, K. J.; Eary, J. F.; Tait, J. F.; Gibson, D. F.; Lewellen, B.; Link, J. M.; Krohn, K. A. Production of [F-18]-fluoroannexin for imaging apoptosis with PET. *Bioconjugate Chem.* **2004**, *15*, 373–379.
(11) Page, R. L.; Garg, P. K.; Garg, S.; Archer, G. E.; Bruland, O. S.; Zalutsky, M. R. PET imaging of osteosarcoma in dogs using a fluorine-18-labeled monoclonal antibody Fab fragment. *J. Nucl. Med.* **1994**, *35*, 1506–1513.
(12) Page, R. L.; Garg, P. K.; Vaidyanathan, G.; Zalutsky, M. R. Preclinical evaluation and PET imaging of ^{18}F-labeled Mel-14 F(ab′)2 fragment in normal dogs. *Nucl. Med. Biol.* **1994**, *21*, 911–919.
(13) Li, J.; Trent, J. O.; Bates, P. J.; Ng, C. K. Labeling G-rich oligonucleotides (GROs) with N-succinimidyl 4-[^{18}F]fluorobenzoate (S^{18}FB). *J. Labelled Compd. Radiopharm.* **2006**, *49*, 1213–1221.
(14) Olafsen, T.; Cheung, C. W.; Yazaki, P. J.; Li, L.; Sundaresan, G.; Gambhir, S. S.; Sherman, M. A.; Williams, L. E.; Shively, J. E.; Raubitschek, A. A.; Wu, A. M. Covalent disulfide-linked anti-CEA diabody allows site-specific conjugation and radiolabeling for tumor targeting applications. *Protein Eng. Des. Sel.* **2004**, *17*, 21–27.
(15) Li, X.; Link, J. M.; Stekhova, S.; Yagle, K. J.; Smith, C.; Krohn, K. A.; Tait, J. F. Site-specific labeling of annexin V with F-18 for apoptosis imaging. *Bioconjugate Chem.* **2008**, *19*, 1684–1688.
(16) Tait, J. F.; Smith, C.; Levashova, Z.; Patel, B.; Blankenberg, F. G.; Vanderheyden, J. L. Improved detection of cell death in vivo with annexin V radiolabeled by site-specific methods. *J. Nucl. Med.* **2006**, *47*, 1546–1553.
(17) Junutula, J. R.; Bhakta, S.; Raab, H.; Ervin, K. E.; Eigenbrot, C.; Vandlen, R.; Scheller, R. H.; Lowman, H. B. Rapid identification of reactive cysteine residues for site-specific labeling of antibody-Fabs. *J. Immunol. Methods* **2008**, *332*, 41–52.
(18) Junutula, J. R.; Raab, H.; Clark, S.; Bhakta, S.; Leipold, D. D.; Weir, S.; Chen, Y.; Simpson, M.; Tsai, S. P.; Dennis, M. S.; Lu, Y.; Meng, Y. G.; Ng, C.; Yang, J.; Lee, C. C.; Duenas, E.; Gorrell, J.; Katta, V.; Kim, A.; McDorman, K.; Flagella, K.; Venook, R.; Ross, S.; Spencer, S. D.; Lee Wong, W.; Lowman, H. B.; Vandlen, R.; Sliwkowski, M. X.; Scheller, R. H.; Polakis, P.; Mallet, W. Site-specific conjugation of a cytotoxic drug to an antibody improves the therapeutic index. *Nat. Biotechnol.* **2008**, *26*, 925–932.
(19) Cai, W.; Zhang, X.; Wu, Y.; Chen, X. A thiol-reactive ^{18}F-labeling agent, N-[2-(4-^{18}F-fluorobenzamido)ethyl]maleimide, and synthesis of RGD peptide-based tracer for PET imaging of alpha v beta 3 integrin expression. *J. Nucl. Med.* **2006**, *47*, 1172–1180.
(20) Berndt, M.; Pietzsch, J.; Wuest, F. Labeling of low-density lipoproteins using the ^{18}F-labeled thiol-reactive reagent N-[6-(4-[^{18}F]-fluorobenzylidene)aminooxyhexyl]maleimide. *Nucl. Med. Biol.* **2007**, *34*, 5–15.
(21) Toyokuni, T.; Walsh, J. C.; Dominguez, A.; Phelps, M. E.; Barrio, J. R.; Gambhir, S. S.; Satyamurthy, N. Synthesis of a new heterobifunctional linker, N-[4-(aminooxy)butyl]maleimide, for facile access to a thiol-reactive ^{18}F-labeling agent. *Bioconjugate Chem.* **2003**, *14*, 1253–1259.
(22) Wuest, F.; Kohler, L.; Berndt, M.; Pietzsch, J. Systematic comparison of two novel, thiol-reactive prosthetic groups for ^{18}F labeling of peptides and proteins with the acylation agent succinimidyl-4-[^{18}F]fluorobenzoate ([^{18}F]SFB). *Amino Acids* **2009**, *36*, 283–295.
(23) Wuest, F.; Berndt, M.; Bergmann, R.; van den Hoff, J.; Pietzsch, J. Synthesis and application of [^{18}F]FDG-maleimidehexyloxime ([^{18}F]FDG-MHO): a [^{18}F]FDG-based prosthetic group for the chemoselective ^{18}F-labeling of peptides and proteins. *Bioconjugate Chem.* **2008**, *19*, 1202–1210.
(24) de Bruin, B.; Kuhnast, B.; Hinnen, F.; Yaouancq, L.; Amessou, M.; Johannes, L.; Samson, A.; Boisgard, R.; Tavitian, B.; Dolle, F. 1-[3-(2-[^{18}F]fluoropyridin-3-yloxy)propyl]pyrrole-2,5-dione: design, synthesis, and radiosynthesis of a new [^{18}F]fluoropyridine-based maleimide reagent for the labeling of peptides and proteins. *Bioconjugate Chem.* **2005**, *16*, 406–420.
(25) Wangler, B.; Quandt, G.; Iovkova, L.; Schirrmacher, E.; Wangler, C.; Boening, G.; Hacker, M.; Schmoeckel, M.; Jurkschat, K.; Bartenstein, P.; Schirrmacher, R. Kit-like ^{18}F-labeling of proteins: synthesis of 4-(di-*tert*-butyl[^{18}F]fluorosilyl)benzenethiol (Si[^{18}F]FA-SH) labeled rat serum albumin for blood pool imaging with PET. *Bioconjugate Chem.* **2009**, *20*, 317–321.
(26) Rosa-Neto, P.; Wangler, B.; Iovkova, L.; Boening, G.; Reader, A.; Jurkschat, K.; Schirrmacher, E. [^{18}F]SiFA-isothiocyanate: a new highly effective radioactive labeling agent for lysine-containing proteins. *ChemBioChem* **2009**, *10*, 1321–1324.
(27) Rostovtsev, V. V.; Green, L. G.; Fokin, V. V.; Sharpless, K. B. A stepwise huisgen cycloaddition process: copper(I)-catalyzed regioselective "ligation" of azides and terminal alkynes. *Angew. Chem., Int. Ed. Engl.* **2002**, *41*, 2596–2599.
(28) Tornoe, C. W.; Christensen, C.; Meldal, M. Peptidotriazoles on solid phase: [1,2,3]-triazoles by regiospecific copper(I)-catalyzed 1,3-dipolar cycloadditions of terminal alkynes to azides. *J. Org. Chem.* **2002**, *67*, 3057–3064.
(29) Marik, J.; Sutcliffe, J. L. Click for PET: rapid preparation of [^{18}F]fluoropeptides using Cu(I) catalyzed 1,3-dipolar cycloaddition. *Tetrahedron Lett.* **2006**, *47*, 6681–6684.
(30) Smith-Jones, P. M.; Solit, D.; Afroze, F.; Rosen, N.; Larson, S. M. Early tumor response to Hsp90 therapy using HER2 PET: comparison with ^{18}F-FDG PET. *J. Nucl. Med.* **2006**, *47*, 793–796.
(31) Smith-Jones, P. M.; Solit, D. B.; Akhurst, T.; Afroze, F.; Rosen, N.; Larson, S. M. Imaging the pharmacodynamics of HER2 degradation in response to Hsp90 inhibitors. *Nat. Biotechnol.* **2004**, *22*, 701–706.
(32) Glaser, M.; Arstad, E. "Click labeling" with 2-[^{18}F]fluoroethylazide for positron emission tomography. *Bioconjugate Chem.* **2007**, *18*, 989–993.
(33) Lewis, W. G.; Magallon, F. G.; Fokin, V. V.; Finn, M. G. Discovery and characterization of catalysts for azide-alkyne cycloaddition by fluorescence quenching. *J. Am. Chem. Soc.* **2004**, *126*, 9152–9153.
(34) Chan, T. R.; Hilgraf, R.; Sharpless, K. B.; Fokin, V. V. Polytriazoles as copper(I)-stabilizing ligands in catalysis. *Org. Lett.* **2004**, *6*, 2853–2855.
(35) Rodionov, V. O.; Presolski, S. I.; Diaz, D. D.; Fokin, V. V.; Finn, M. G. Ligand-accelerated Cu-catalyzed azide-alkyne cycloaddition: a mechanistic report. *J. Am. Chem. Soc.* **2007**, *129*, 12705–12712.

(36) Rodionov, V. O.; Presolski, S. I.; Gardinier, S.; Lim, Y. H.; Finn, M. G. Benzimidazole and related ligands for Cu-catalyzed azide-alkyne cycloaddition. *J. Am. Chem. Soc*. **2007**, *129*, 12696–12704.
(37) Devaraj, N. K.; Keliher, E. J.; Thurber, G. M.; Nahrendorf, M.; Weissleder, R. ^{18}F labeled nanoparticles for in vivo PET-CT imaging. *Bioconjugate Chem*. **2009**, *20*, 397–401.
(38) Sereikaite, J.; Jachno, J.; Santockyte, R.; Chmielevski, P.; Bumelis, V. A.; Dienys, G. Protein scission by metal ion-ascorbate system. *Protein J*. **2006**, *25*, 369–378.
(39) Sen Gupta, S.; Kuzelka, J.; Singh, P.; Lewis, W. G.; Manchester, M.; Finn, M. G. Accelerated bioorthogonal conjugation: a practical method for the ligation of diverse functional molecules to a polyvalent virus scaffold. *Bioconjugate Chem*. **2005**, *16*, 1572–1579.
(40) Ward, J. F.; Johansen, I.; Aasen, J. Radiosensitization by N-ethyl maleimide—a model chemical system. *Int. J. Radiat. Biol. Relat. Stud. Phys. Chem. Med*. **1969**, *15*, 163–170.
(41) Hayon, E.; Simic, M. Radiation sensitization reactions of N-ethylmaleimide with model compounds. *Radiat. Res*. **1972**, *50*, 464–478.
(42) Solit, D. B.; Zheng, F. F.; Drobnjak, M.; Munster, P. N.; Higgins, B.; Verbel, D.; Heller, G.; Tong, W.; Cordon-Cardo, C.; Agus, D. B.; Scher, H. I.; Rosen, N. 17-Allylamino-17-demethoxygeldanamycin induces the degradation of androgen receptor and HER-2/neu and inhibits the growth of prostate cancer xenografts. *Clin. Cancer Res*. **2002**, *8*, 986–993.
(43) Wilson, A. A.; Jin, L.; Garcia, A.; DaSilva, J. N.; Houle, S. An admonition when measuring the lipophilicity of radiotracers using counting techniques. *Appl. Radiat. Isot*. **2001**, *54*, 203–208.